

Inhibition of Bacterial Biofilms in Microfluidic Chambers

Master in Molecular Biology and Biomedicine

University of Cantabria and University of the Basque Country

Institute of Biomedicine and Biotechnology of Cantabria (IBBTEC)

Author: María Fernández de Landa Albaina

Supervisor: Raúl Fernández López (IBBTEC)

June - 2018

Abstract

Bacterial biofilms are a frequent source of infection, colonizing catheters, prosthesis and other medical equipment. Because biofilms are resilient to adverse environmental conditions and protect bacteria against antibiotic treatment, they have proven particularly refractory to treatment; constituting a major health problem in the clinical setting. For these reasons, there is ample interest in developing compounds able to prevent their formation. Conjugative plasmids are known to increase biofilm formation rates, probably due to the adhesive capabilities of the conjugative pilus. Here, we investigate the ability of 2-hexadecynoic acid (2-HDA), a compound known to inhibit bacterial conjugation, to prevent biofilm formation. For this purpose, we fabricated a microfluidic device able to undergo continuous flow, which we investigated two flow velocities: at 8 $\mu\text{l}/\text{min}$ and 10 $\mu\text{l}/\text{min}$, and monitored biofilm formation in continuous time. Image analysis of 22-h time lapse videos revealed the inhibitory effect of 2-HDA on plasmid-mediated biofilm formation in the bacterium *E.coli* as well as a reduction of the biofilm due to the flux velocity.

Keywords: Microfluidics, biofilm, conjugative plasmids, conjugative inhibitors, flux

Contents

1	Background	3
1.1	Biofilms, conjugative plasmids and conjugative inhibitors	3
1.2	Microfluidics	8
2	Objectives	10
3	Experimental methods	10
3.1	Lithography: Wafer Printing	10
3.2	Microfabrication	12
3.3	Bacteria inoculum	14
3.4	Microfluidics	15
3.5	Data Analysis	18
4	Results	18
4.1	Biofilms grown at 8 $\mu\text{l} / \text{min}$	20
4.2	Biofilms grown at 10 $\mu\text{l} / \text{min}$	22
5	Discussion	27
6	Conclusions	30
7	Acknowledgements	30
8	References	31

1 Background

1.1 Biofilms, conjugative plasmids and conjugative inhibitors

Biofilms are an aggregation of prokaryotic cells enclosed in a matrix and attached to a surface, found in wet environments [7, 12] (G. Sharma *et al.*, 2016; L. Hall-Stoodley *et al.*, 2004). Evidence has proven through fossils that biofilms have existed since 3.3 billion of years ago. They are complex systems that have found survival strategies throughout the years against harmful factors such as harsh environmental conditions (temperatures, pH, UV light...) or chemical factors [12](L. Hall-Stoodley *et al.*, 2004).

The most characteristic part of the biofilms, which distinguishes it from planktonic cells, is the protective extracellular polymeric substance (EPS) matrix that is formed above them. This layer is formed on the later stages of the biofilm life, and is made out of water ($\approx 97\%$), polysaccharides, proteins, nucleic acids, nutrients, lipids / phospholipids. The polysaccharides provide structural support for the biofilm and consists on three types of exopolysaccharides: *colanic acid*, responsible for protection of the biofilm against stress related to environmental conditions; *cellulose*, in charge of structural support; and *PGA* (β -1,6-*N*-acetyl-*D*-glucosamine polymer), accountable for the interaction between cells and with the surface. This matrix not only provides protection against hostile environments and toxic molecules, but also provides a stable zone in which the bacteria can multiply. Inside the matrix, nutrients and enzymes are concentrated and quorum sensing communication molecules coordinate its behavior [1, 7, 12] (C. Beloin *et al.*, 2008; G. Sharma *et al.*, 2016; L. Hall-Stoodley *et al.*, 2004). The structure of the biofilm depends as well on external factors like nutrients and the flow regime of the wet environment in which it sits.

The biofilm life can be divided into various stages, in which depending on the author the number may vary. [1, 7, 12] (C. Beloin *et al.*, 2008; G. Sharma *et al.*, 2016; L. Hall-Stoodley *et al.*, 2004) Here we will divide the stages into 4 phases as G. Sharma *et al.*, which can be seen in Fig. 1:

1. **Initial aggregation.** Here the bacteria begin to attach themselves to the surface which can be biotic, i.e other cells in tissues, or abiotic, i.e metal, steel, implants... This stage depends on environmental factor and specific bacterial genes
2. **Early development.** The bacteria begin to aggregate themselves and become sessile.

Here the adhesive structures are induced and development of the biofilm and begin to enhance the cell-cell and the cell-surface interaction.

3. **Maturation.** In this stage the EPS and autotransporters, which help cell-cell interaction) create the biofilm with the protective matrix.
4. **Dispersion.** It is when the biofilm matrix breaks and the cells are dispersed. This could be a result form enzymatic degradation or a coordinated detachment mediated by quorum sensing molecules

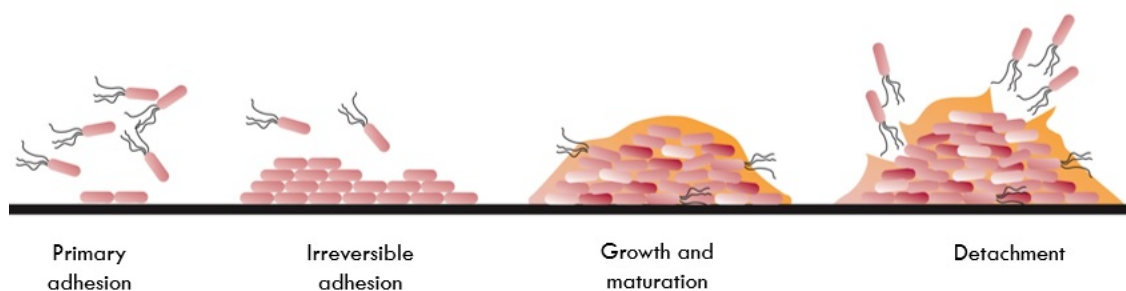


Figure 1: Representation of the four stages of evolution of a biofilm. [7] (G. Sharma *et al.*, 2016)

There are two major interrelated factors that help the formation of biofilms: pili and plasmids. The pili are hairlike filaments that are found on the surface of the bacteria which can be divided into two structures important for the development of bacterial biofilms are Type IV pili and conjugative pili. The Type IV pili is in charge of the motility and to cell-cell / cell-surface interactions of the bacteria. The second pili is responsible for the DNA transfer between bacteria, denominated bacterial conjugation. Conjugative plasmids are self-transmissible. They move from donor to recipient, and encode all genes needed for their own transfer. Conjugative pili are essential for the process of conjugation. They also mediate bacteria adhesion, thus promote biofilm formation.

Bacterial conjugation takes place in two phases: plasmid DNA is mobilized by MOB genes and DNA is transported through the conjugative pili. Conjugative and non-conjugative plasmids has been studied since the 1990s whether it affected the formation of biofilm or not. These studies proved that both plasmids were capable of inducing biofilm [1](C. Beloin *et al.*, 2008). In the early millennium, Ghigo studied whether the conjugative DNA of the plasmid was relevant to the formation of biofilms. His result was that repressed plasmids did not form biofilms in absence of F-pilus. He demonstrated that the F-pilus has a key role in the

adhesion of the bacteria to the surfaces and accelerated the formation of the biofilm. He also found that, by adding a small population of donor bacteria with the conjugative pili into a larger population of plasmid free strains, biofilm would form. This last observation proved that that conjugation and biofilm formation are intimately linked [11] (J.M. Ghigo, 2001). Since conjugation mediates the spread of antibiotic resistance genes, and biofilms protect bacteria from treatment, this association is a major clinical problem.

In a previous study done in the laboratory, where they studied the R100-1 conjugative plasmid, which will also be investigated in this work, and saw that it quadrupled the optical density of biofilm formed by the BW25113 E.coli, (Fig. 2) in a static environment. Here the effect of this conjugative plasmid will be tested in two different continuous uniform flows.

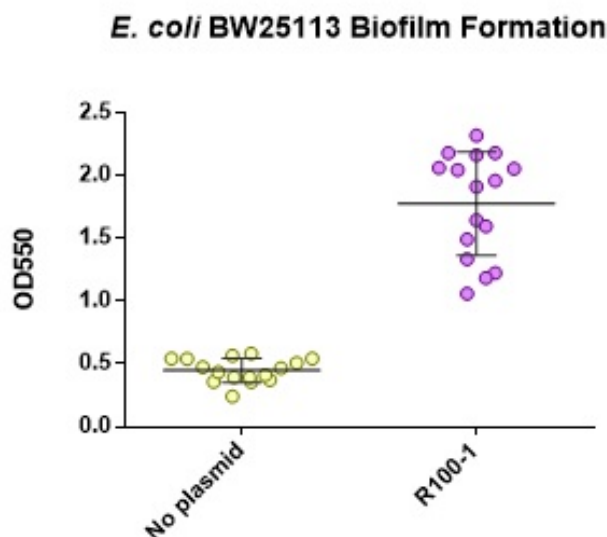


Figure 2: Optical density (OD) at 550 nm of the biofilms formed with and without the conjugative plasmid R100-1.

The co-occurrence of antibiotic resistance and biofilm formation has yielded many infections nearly intractable by traditional antibiotics. Therefore, there is ample interest in developing strategies against these two problems.

One of the routes is to prevent the adhesion of the bacteria in the first stages of the biofilm formation. Here, this factor can be studied through the material of the surface where the bacteria lays or through the pili that favor the adhesion to the surface. In the first case, it could be a medical solution since most of the biofilms in a body are formed in catheters,

prosthesis, i.e external, non-biologic materials that are inserted into the body. [2] (Beloin *et al.*, 2014) The prevention of adhesion by targeting the pili or the plasmids is defined by molecules defined as conjugative inhibitors, which we will explain further below.

Another way is to intervene in the biofilm by cutting its maturation, in other words, in the last phases of the biofilm evolution. Here the mechanisms against quorum sensing, using screening factors like nanoparticles, like nitric oxide, silver or enzyme degradation, have been proposed and have shown good results. [2, 7] (C. Beloin *et al.*, 2014 ; G. Sharma *et al.*, 2016)

The solution to the biofilm formation that we are studying here is the function of the conjugative inhibitors (COINs), which specifically reduce or abolish bacterial conjugation, without killing donor or recipient bacteria. Unsaturated fatty acids have been found to be specific COINs. Molecules with different moieties have proven effective. In this work we will use the synthetic COIN 2-hexadecynoic acid. (2-HDA). 2-HDA blocks conjugation in different plasmid groups. Its molecular target seems to be the conjugative apparatus. It specifically binds TrwD, an essential ATPase. However other targets are likely, since 2-HDA also inhibits F-like plasmids (like R100), which lack a TrwD homolog.[6, 13](E. Cabezón *et al.*, 2017; M. Getino *et al.*, 2015)

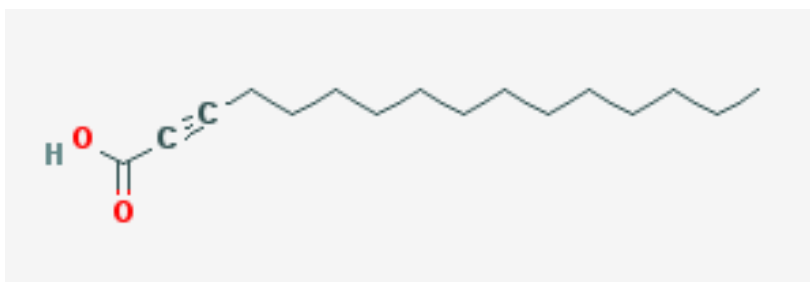


Figure 3: 2-hexadecynoic acid molecule. $C_{16}H_{28}O_2$ [14](NCBI, 2018)

2-hexadecynoic acid is a synthetic fatty acid composed of a carboxylic group, a triple bond and a long carbon chain, as seen in Fig. 3. In a study made by M. Getino *et al.* they found that the ideal conjugative inhibitors have a long, unsaturated chain with a OH group in one end, and that the 2-HDA had the optimal carbon chain length. In this study, the effect of the inhibitor was noted when the donor cells were preincubated in the 2-HDA, when the recipient bacteria grew with the inhibitor there were no changes in comparison with the

control group, as seen in Fig. 4.A. Later, various strains of bacteria including *E. coli*, were used to see the effect of the 2-HDA on plasmid conjugation frequency, seen in Fig. 4. B. The decrease in the conjugation frequency observed in several different species proved that 2-HDA is an effective conjugation inhibitor. [13] (M. Getino *et al.*, 2015)

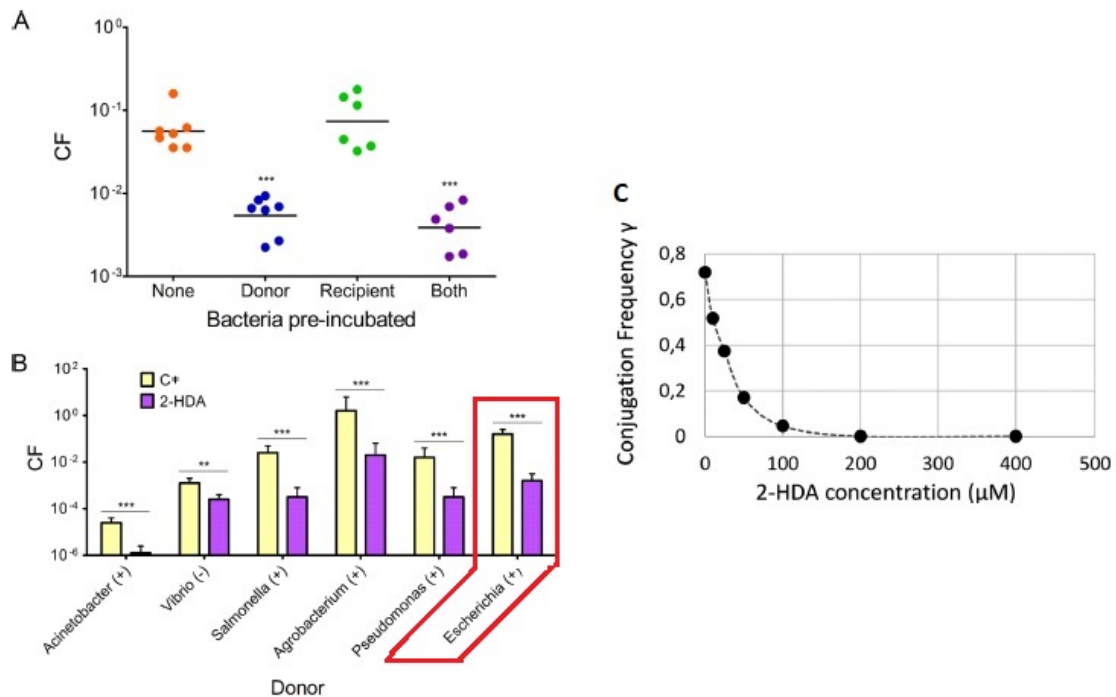


Figure 4: In A and B the effect of the 2-HDA in the donor cells is shown. A) The conjugation frequencies (CF) are shown in the cases of the COIN added to the donor, recipient cells or both. B) The CF of different hosts, including *E. coli* surrounded in red, with and without the 2-HDA. Both representations are done on a logarithmic scale. C) Values of the CF of R1drd19 against the concentration of 2-HDA (in μM). [13] (M. Getino *et al.*, 2015)

There is preliminary evidence showing that 2-HDA is also able to block plasmid-induced biofilm formation. When the optical density of an R100 induced biofilm was tested in a static environment, a sharp reduction was observed in samples treated with 2-HDA, as seen in Fig. 5.

In this experiment, we will study the density of the biofilm formed by the R100-1 plasmid, with and without the 2-HDA conjugative inhibitor, but in a continuous flow environment, i.e. non static nutrients, by using a microfluidic setup.

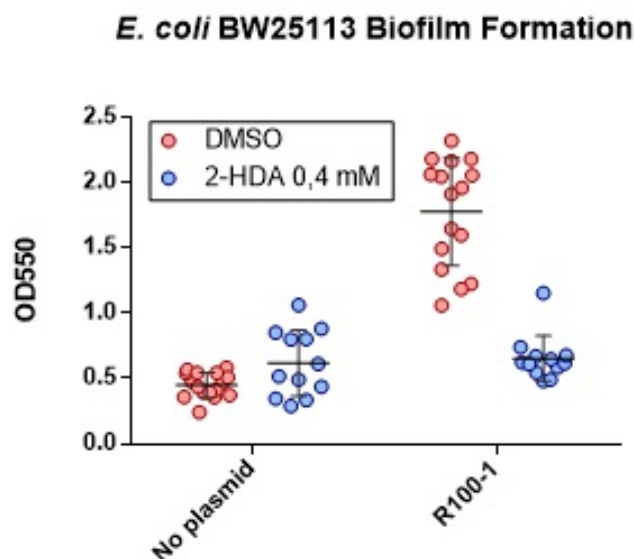


Figure 5: Study where the optical density (OC) at 550 nm is studied of the biofilm formation with and without the conjugative plasmid R100-1 (in red). Next to it, in blue, the density of the biofilms under the effect of the 2-HDA COIN.

1.2 Microfluidics

Microfluidics is a field where fluids are manipulated and studied at a microscale, used in engineering, chemistry, medicine and biology. This technology is suited for the study of bacterial biofilms ([8]-[10]) since the environmental conditions can be controlled and changed at will. In this study, biofilms will grow in a *chip* with a milimetric structure, seen in Fig. 7 with a continuous flow of nutrients passing through it.

Microorganism growth studies have been traditionally carried out *in vitro* experiments and through animal testing. Although both methods have been proven to have a success rate, they have many disadvantages. Microorganisms have short lifespans when grown in Petri dishes due to the lack of new nutrients, typically only lasting three days. These volumes are usually too big to observe the individual growth and it is very hard to control all aspects of the environment, which does not always favor the bacterial growth.

Additionally, animal testing is associated to high costs and slow data recollection. Most importantly sometimes it fails to give a viable prediction of the response on humans, and may lead to moral and ethical issues. Microfluidics has numerous advantages when studying microorganisms seen in Fig. 6 such as [4](D. Huh *et al.*, 2012):

1. The human body can be better simulated since it is easier to imitate the conditions and variables of the human body (flow velocity, temperature, nutrient concentration, etc.). The fluids and nutrients that are injected can be controlled on a submillimetric scale precisely and be manipulated by controlling the fluid pressures.
2. Low cost relative to other methods due to the chips being fabricated in a similar fashion.
3. The transparency of the chips helps the observation and can be recorded in real time.
4. The method can mimic the environment, the bacteria live longer, and enables independent 3D bacterial growth.
5. It can simulate high and low throughput analysis.
6. It needs less volume of bacteria, nutrients, etc. to obtain the results and, since the experiment is done on a smaller scale, the data analysis is faster.

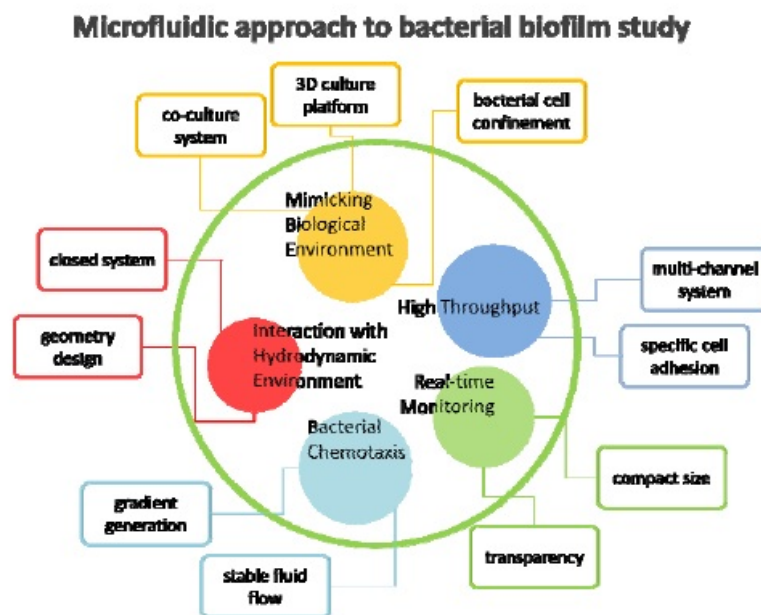


Figure 6: Diagram of most of the advantages that microfluidics has to study the evolution of microorganisms. [4](D. Huh *et al.*, 2012)

This experiment is carried out with a millimetric chip made of polydimethylsiloxane (PDMS), a transparent, elastic polymer, with a fixed temperature, light, pressure and flow environment (see section 3).

2 Objectives

The overall goal of this project is to test whether conjugation inhibitors may be used to prevent biofilm formation. For this purpose, we intended to:

1. Develop an experimental setup to test biofilm formation under continuous and regulatable flow in microfluidic chambers.
2. Test whether conjugative plasmids induced biofilm formation in this setting.
3. Test whether conjugation inhibitors may be used to prevent biofilm formation.

3 Experimental methods

This section includes the experimental procedures required for i) fabrication of the microfluidic chamber, ii) operation of the microfluidic chamber and iii) measurement and quantitation of biofilm production.

3.1 Lithography: Wafer Printing

The first part of the process was to obtain the chip with which we would work with. This phase included designing and fabrication of the microfluidic wafer and PDMS soft lithography. The chamber employed was based on the design described in [10] (J.L Song *et al.*, 2014). The overall design was re-dimensioned to fit in the field of view of our microscopic setup (see section 3.4). Re-scaling maintained the overall aspect ratios of the original design.

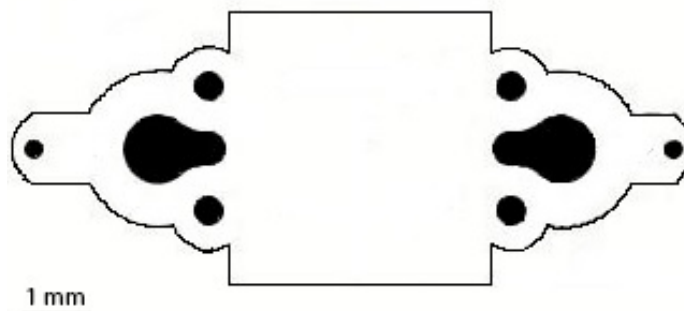


Figure 7: The rescaled design of the chip used in the experiment based on [10] (J.L Song *et al.*, 2014) with the scale at the bottom.

This was sent to Micrux Technologies, a firm specialized in lithography, that created the wafer seen in Fig. 9.

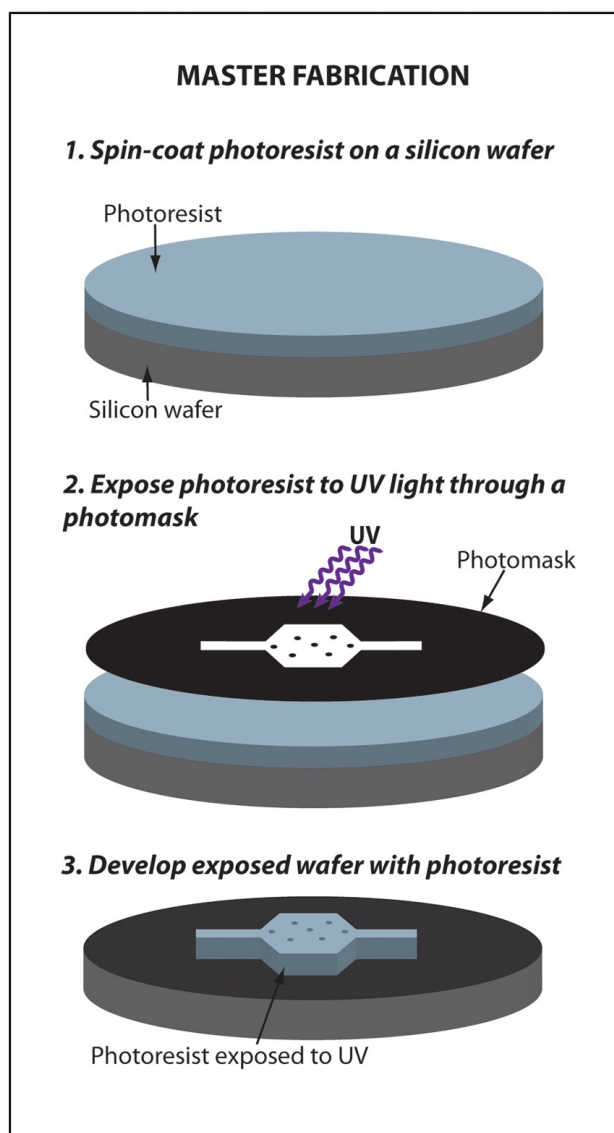


Figure 8: Summary of the wafer fabrication process in which the silicon wafer is photo-coated, exposed to UV light with a photomask and then cleaned where the final design is permanently placed. [15] (A. San Miguel & H. Lu, 2013)

In Micrux Technologies, a process called photolithography is used to create the wafer. Here on a silicon wafer a substrate with a photo sensitive polymer, denominated photoresistor, was covered while it was on a spin-coater. Afterwards, it was covered by a photomask, which is a plate made out of quartz plate with microstructures. This was then exposed to UV light, where the photomask could become more or less resistant, where the design of the photomask passed to the photoresistor. Finally, the photomask with the excess of photoresistor were taken off of the wafer, leaving the wafer with the design of our chip., as seen in Fig. 8. This process is highly expensive but used often to create microelectric circuits,



Figure 9: Silicone wafer used to microfabricate the microfluidic chips. The design is repeated 9 times to obtain a large number of chips in the process.

microanalytical devices amongst other devices. It cannot be used in curved surfaces and the range of materials where it can be used is very low. [5] (D. Quin *et al*, 1998)

3.2 Microfabrication

Once the wafer was obtained, it was silanized to avoid the PDMS getting adhered on it and breaking it. The process was handled under a fume hood, since trichloro perfluorooctyl silane is toxic. In the hood we covered the base with two layers of aluminum foil, the first one covered all of the base, and a smaller second piece, where the wafer was placed, was put on top. Two drops of silane were put in a corner of the second layer of foil next to the wafer and a vacuum desiccator lid covered them to create a closed environment. We waited for 15 minutes so the silane evaporated and the gas covered the surface.

Afterwards, the wafer was put on a 150 °C hotplate in the fume hood for 10 minutes, so the silane could cure and the excess would evaporate. [3](C. Saenz , 2015). After this step, the wafer could be used to microfabricate the chips.

Microfabrication took place in a semi-white room, in a laminar flow hood to avoid interference from dust or any debris. In order to avoid any fibers from contaminating the chip manufacture, we had to wear full body covers, gloves and a protection screen.

PDMS (polydimethylsiloxane) was mixed in a laminar-flow hood with a curing agent in a

45: 4.5 g proportion and put in a vacuum oven for 30 min at room temperature to remove bubbles created during the mixing. While the mix was in the chamber, a crystal petri dish was covered with aluminum foil, making sure it covered all of the surfaces, and then, the wafer was placed inside. Afterwards, the mix was poured on the wafer, and was put into the oven again (Fig.10a) for another 30 min. This process eliminated the rest of air bubbles in the PDMS mix that would influence negatively in the next phase. Once this was finished, the mold was incubated in a normal oven at 65°C overnight. An outline of the fabrication process is shown in Fig. 11.1.

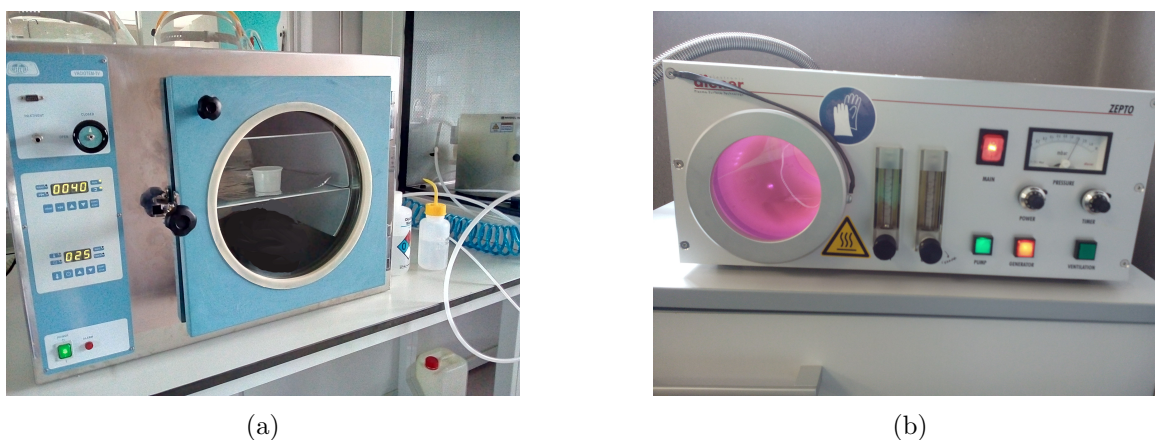


Figure 10: The vacuum oven (a) used to clear the bubbles from the PDMS mix and the O₂ plasma generator that made the plasma to stick the chip to the crystal slide.

The following day, PDMS had solidified into a flexible polymer surface. The aluminum foil was taken out of the dish and the PDMS was peeled off the wafer, and each chip was cut out individually. Each chip was then punctured with a 0.5 mm punch, at the two distant points along the longest axis of the chip, creating an input and an output hole from the chip chamber. Next, the chips were cleaned with isopropyl alcohol, dried with an air pistol and put on a laboratory slide (that was cleaned with isopropyl), as shown in Fig. 11.2. Also a crystal coverslip was cleaned with ethanol, isopropyl alcohol, water and isopropyl alcohol, in that order and then dried with the air pistol as well. One pair of the cover and the slide with the PDMS chip were put into an O₂ plasma generator (Fig.10b), in a way where the slide took up a small part of the coverslip so it would not fly into the machine, seen in Fig. 11.3. In order to operate the generator, first vacuum was needed. The pressure had to drop to 0.24 ± 0.02 mbar. At this pressure, plasma generation was ignited. A bright purple glowing in the chamber was indicative of plasma generation. The chips and coverslips were subjected to plasma for 30-60 seconds. Finally, after taking both objects out of the plasma generator, they

were taken to the hood where the chip and crystal cover slip were sealed together, Fig.11.4 and put into the oven at 65°C overnight. The full process of fabrication of the chips took 48 h.

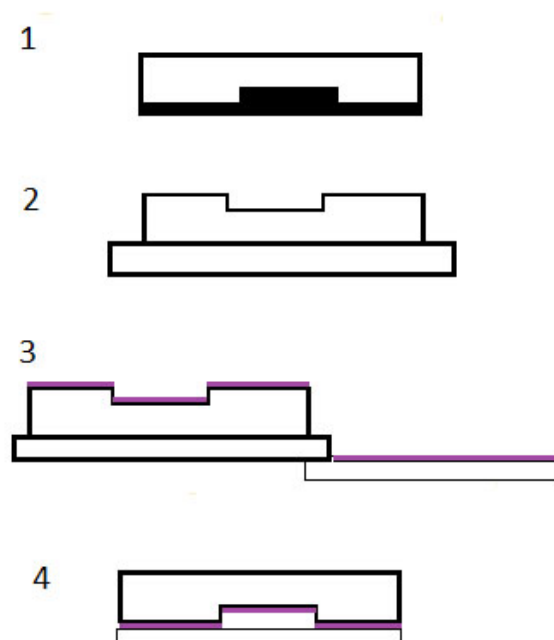


Figure 11: Outline of the microfabrication process. 1- The process in which the wafer (seen in black) was covered by the PDMS (in white) and it took its shape. 2- The PDMS chip, once it was cut, was cleaned with isopropanol and placed on a clean coverslip. 3- The PDMS chip and a clean crystal slip were inserted into the O₂ plasma generator, making sure that the edge of the crystal was covered by the coverslip so it would not be blown away and the plasma (the purple line) was perched on the top surfaces 4- Both objects were placed and glued together with the plasma creating a small space where the bacteria would grow.

3.3 Bacteria inoculum

On the first day, in a laminar hood cabinet, to ensure sterile conditions, 0.1 ml of *E.coli* cells were inoculated into 10 ml Erlenmeyer flask filled with Luria-Bertani rich medium (LB). Bacteria were allowed to grow overnight by incubating the flask at 37°C under gentle agitation. We used two different strains to perform our experiments.

- *E.coli* Bw25113. This strain was used as the negative control without conjugative plasmid. Genotype: D(araD-araB)567 lacZ4787 (::rrnB-3) D(araH-araF) ::FRT D(araE)::FRT D(rhaD-rhaB)::FRT hsdR514
- *E.coli* Bw25113 R100-1. Strain containing the F-like de-repressed conjugative plasmid R100.

Strains were supplemented with appropriate antibiotic concentrations (Cloramphenicol 25 micrograms/ml, Rifampicine 20 micrograms/ml).

When appropriate, the conjugation inhibitor 2-HDA was used at a final concentration of 2 mM.

Overnight cultures were washed twice in fresh LB media prior to their inoculation in the microfluidic chambers.

Finally, to provide uniformity, the optical density ($O.D$) was measured and adjusted to 4, which would mean in the volume we would have 10^{8-9} bacterial cells. To do that, an electrophotometer was used to measure the optical density ($O.D_1$) of 1ml of LB, for calibration, and a 10% dissolution of culture. Afterwards, to assure the optical density, a 1.5 ml dissolution was made with the corresponding volumes using the following formula:

$$O.D_1 V_1 = O.D_2 V_2 \rightarrow C_1 V_1 = V_2 \cdot 4 \quad (1)$$

Where V is the final volume. V_1 was the volume of strain dissolution needed to obtain $O.D$ of 4.

When the inhibitor was used, 2-HDA was added at a final concentration of 0.3 mM to the inoculum and to the LB.

3.4 Microfluidics

The experimental setup for this experiment was made of 2 pumps, a microscope, a photo camera, a heat chamber, a computer, a transparent 2 cm thick metacrylate block, various syringes, a filter and various 0.3 mm diameter tubes and adapters, as shown in Fig. 12 and Fig. 13.

The heat chamber was covered entirely with black cardboard to avoid the background light to interfere with our optical density measurements.

Before each experiment, tubing was cleaned with isopropanol and sterile water. For this purpose, a syringe was filled with a solution of isopropanol at 0,7 M and put into the input syringe. The isopropanol was pushed through manually for a minute. Next, with the

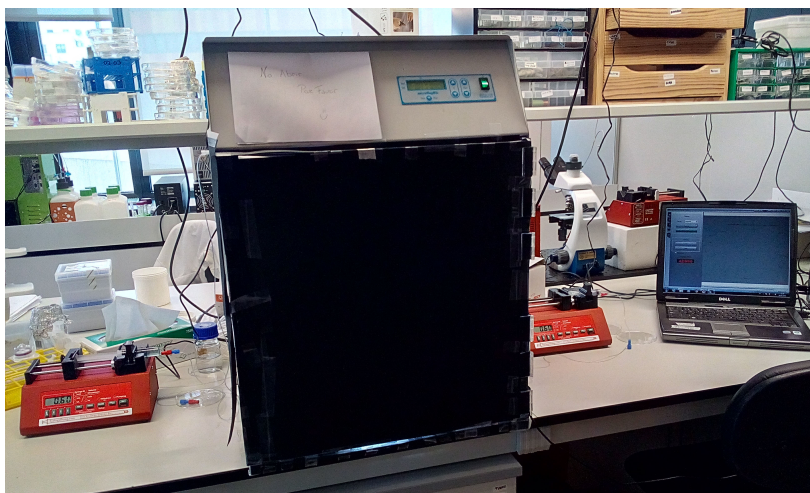


Figure 12: Photograph of the setup used in the microfluidic part of the experiment. The heat chamber covered in black cardboard is in the center (which contained the microscope and the camera seen in Fig. 13). Beside it the two pumps can be seen with the syringes and the tubes. Finally on the right side of the image, the computer where the images were taken and stored.

same syringe, the same process was done with the output tube. Afterwards, with a different syringe, sterile water was pushed through the tubes, to eliminate any rests of the alcohol.

After cleaning the tubes, the light at the base of the microscope was turned on to the maximum ($6.19 \pm 0.01 \mu\text{M}$), so no environmental light would change the conditions in the growth of the bacteria nor the recording of data. Also a transparent 2 cm thick block of metacrylate was put between the microscope and the petri dish. This was done so the heat of the light at the base of the microscope could not affect the bacterial growth of the chip. Then the camera was turned on and the chip was placed so the center of the chip would be in the center of the image. When the chip was in position, it was taped to the petri dish, which was also taped to the metacrylate block.

Once everything was in place, the input and output tubes were inserted in the holes of the chip and LB with Crystal Violet (0.01%w/v) was inserted from a syringe at $27 \mu\text{l}/\text{min}$ with an automatic pump. To eliminate air bubbles within the circuit, we employed dead-end filling. For this purpose, we set up an input flux of $27 \mu\text{l}/\text{min}$, while the output flux was blocked. This allowed air trapped to exit the circuit through the porous PDMS.

When there were no bubbles, the clip was removed and the output pump was turned on and set at $27 \mu\text{l}/\text{min}$. If no further bubbles were formed, the pumps would be left running

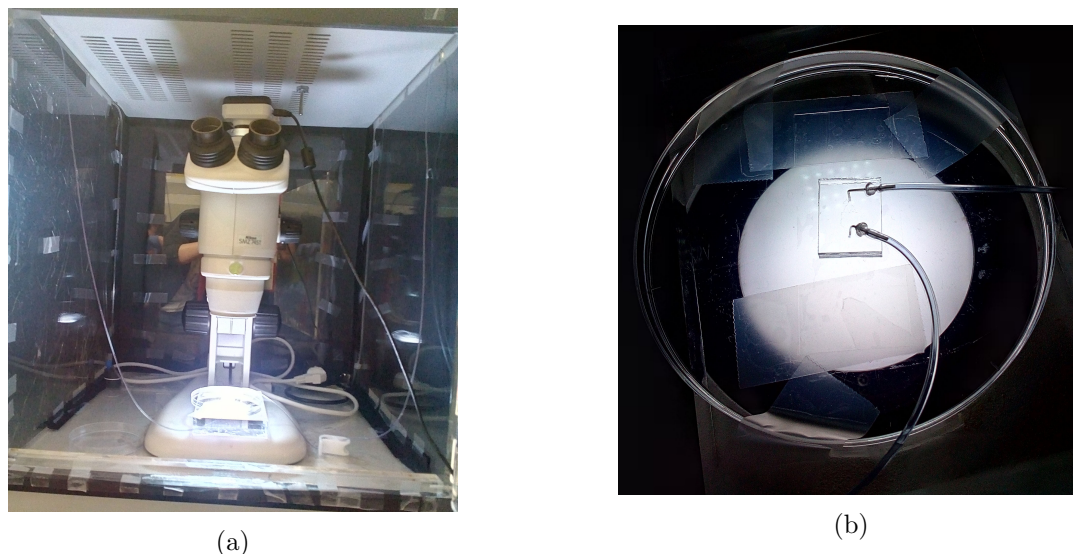


Figure 13: Photographs of the inside of the darkened heat chamber, in (a) the microscope inside the heat chamber with the camera, the metecrylate block, the petri dish and the chip connected to the tubes are shown. In (b) the microfluidic chip can be seen taped to the petri dish and connected to the input and output tubes.

while the next step was carried out. If a bubble formed when the clip was removed, the output tube was re-closed until the bubbles would leave.

While both pumps were running, a 1ml syringe was filled with the bacteria inoculum, and it was made sure that there were no bubbles in it. Afterwards, the pumps were halted and the input and output tubes were removed from the chip. Next, the bacteria were injected into the chip through the input and output holes, in that order, slowly and making sure no bubbles were formed in the process. It was then left 5 minutes so the bacteria would settle on the bottom of the chip.

After bacteria were allowed to settle on the chip, the input syringe was substituted with a 15 ml syringe filled with LB +0.01 %w/v crystal violet. For experiments testing the effect of the conjugation inhibitor 2-HDA, this compound was included in the input syringe at 2mM final concentration. The pump was turned on so any bubbles formed during the switch would not affect the recording of the data.

Finally, the tubes with the LB were reconnected to the chip, and the pumps were turned on at $8 \mu\text{l}/\text{min}$. The camera was turned on and set to take one photograph every 2 minutes. After approximately 22 h, the pumps and the heat chamber were turned off, the syringes

were thrown away and the images were saved in a different folder for each day. Then the tubes were cleaned with isopropanol and sterile water and the metacrylate block was taken away from the heat chamber so it could cool off.

Every time the strain was changed, the entire circuit was sterilized using Virkon(R) and 70% ethanol. The circuit was then flushed thrice to remove any residues of the sterilizing procedure.

This procedure was then repeated with a flux velocity of $10 \mu\text{l} / \text{min}$.

3.5 Data Analysis

Once all of the images were stored in a folder, they were processed with ImageJ [©] (FIJI). To quantify the intensity of biofilm formation, crystal violet signal was transformed into an 8-bit intensity scale. For this purpose, RGB images were transformed into monochrome 8 bit using FIJI. Quantitation was performed on a standard squared region of interest (ROI) so all videos could be pairwise compared.

When the ROI was selected an intensity surface plot was obtained taking into account the grey scale. Since the Crystal-violet stains only the biofilm, the darkness of the image is proportional to the density of biofilm present in the area. The quantitation was produced by taking into account the integrated density of all the images use and then plotted to compare the evolution of the strains.

4 Results

In this section, the compilation of videos of the biofilm growth are displayed in Tab. 1 which can be observed through hyperlinks in the PDF version. With these videos, the integrated density of the bacteria was registered thought time and represented in Fig. 18 and 23.

Date	F/ $\mu\text{l} \cdot \text{min}^{-1}$	Strain	Total Chip Video	2D Video Link	3D Video Link
180503	8	BW25113 + R100-1	180503 chip	180503 spectrum	180503 surface plot
180505	8	BW25113 + R100-1	180503 chip	180505 spectrum	180505 surface plot
180518	8	BW25113 + R100-1 + 2-HDA	180518 chip	180518 spectrum	180518 surface plot
180522	8	BW25113 + R100-1 + 2-HDA	180522 chip	180522 spectrum	180522 surface plot
180517	8	BW25113	180517 chip	180517 spectrum	180517 surface plot
180528	10	BW25113 + R100-1	180528 chip	180528 spectrum	180528 surface plot
180529	10	BW25113 + R100-1	180529 chip	180529 spectrum	180529 surface plot
180530	10	BW25113 + R100-1 + 2-HDA	180530 chip	180530 spectrum	180530 surface plot
180531	10	BW25113 + R100-1 + 2-HDA	180531 chip	180531 spectrum	180531 surface plot
180604	10	BW25113	180604 chip	180604 spectrum	180604 surface plot
180607	10	BW25113	180607 chip	180607 spectrum	180607 surface plot

Table 1: Representation of the growth of the biofilms. The first video is the combination of all the photos obtained in the 22h that lasted the experiment, in black and white. Afterwards, the rectangular section of the chip is selected as region of interest (ROI) and it is reedited with a color spectrum to observe the evolution of density as a 2D and 3D videos, and study the increase if biofilm though time in all of the area. Each video is divided by the date of the experiment and the E.coli strain. The date of the experiment is denominated with the yymmdd format and also applies to the name of the experiment.

4.1 Biofilms grown at $8 \mu\text{l} / \text{min}$

Here the results of the evolution of the biofilms studied at $8 \mu\text{l} / \text{min}$ are displayed. In Fig. 14 the representation on example of the evolution of biofilm is shown through a sequence of photographs taken every 3.15 hours approximately, to display the differences of the conjugative plasmid (Fig. 19a) and the conjugative inhibitor (Fig. 19a), together with the control group (Fig. 14c). Afterwards, in Fig. 15-17 the last photographs of the surface plots acquired from all of the experiments, which represent the density growth of the biofilms, are shown.

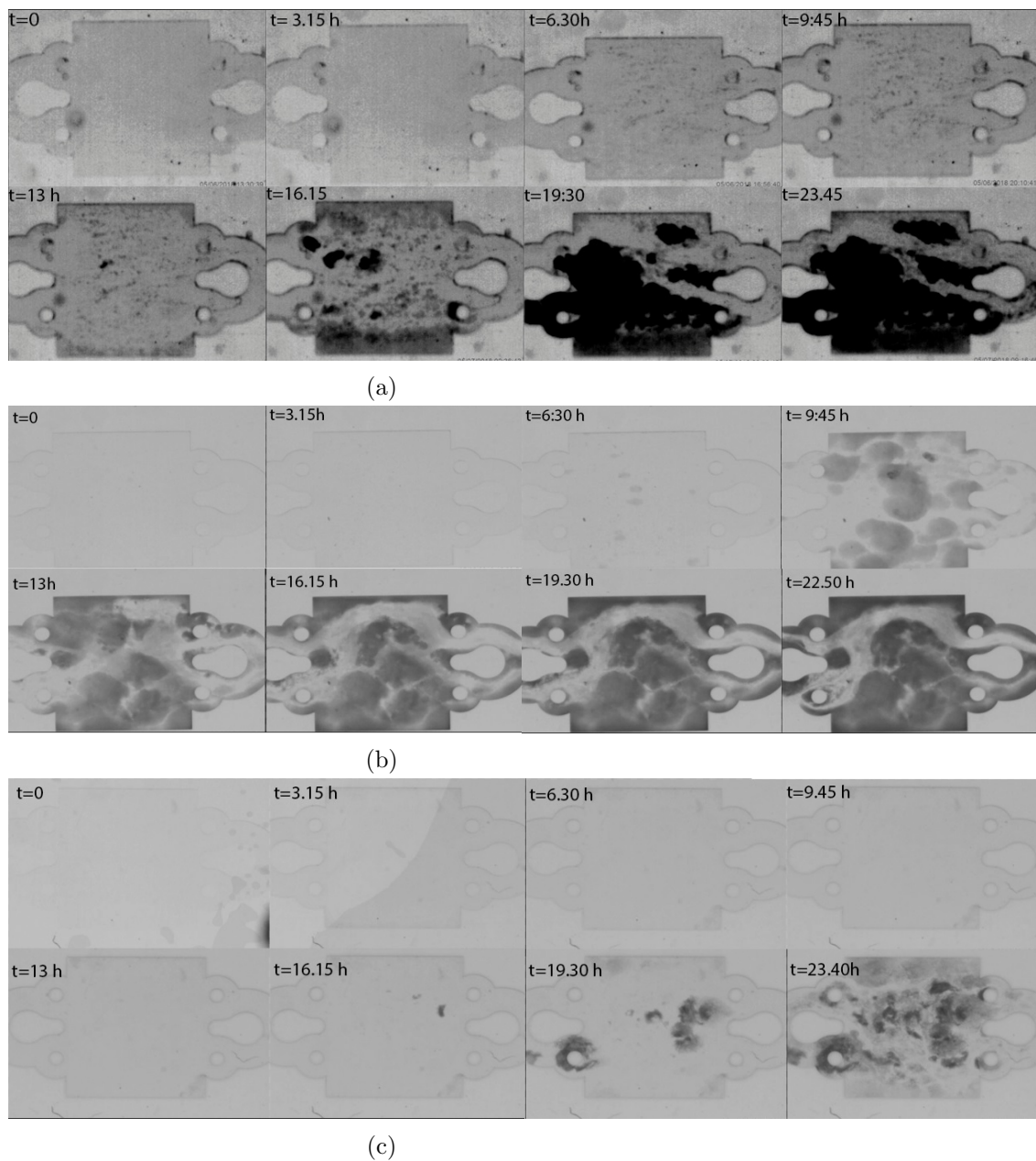


Figure 14: Combination of 8 photographs taken every 3.15 hours approximately from BW25513 strains with : (a) R100-1 conjugative plasmid, (b) 2-HDA conjugative inhibitor and (c) control group subjected to a $8 \mu\text{l} / \text{min}$ flux.

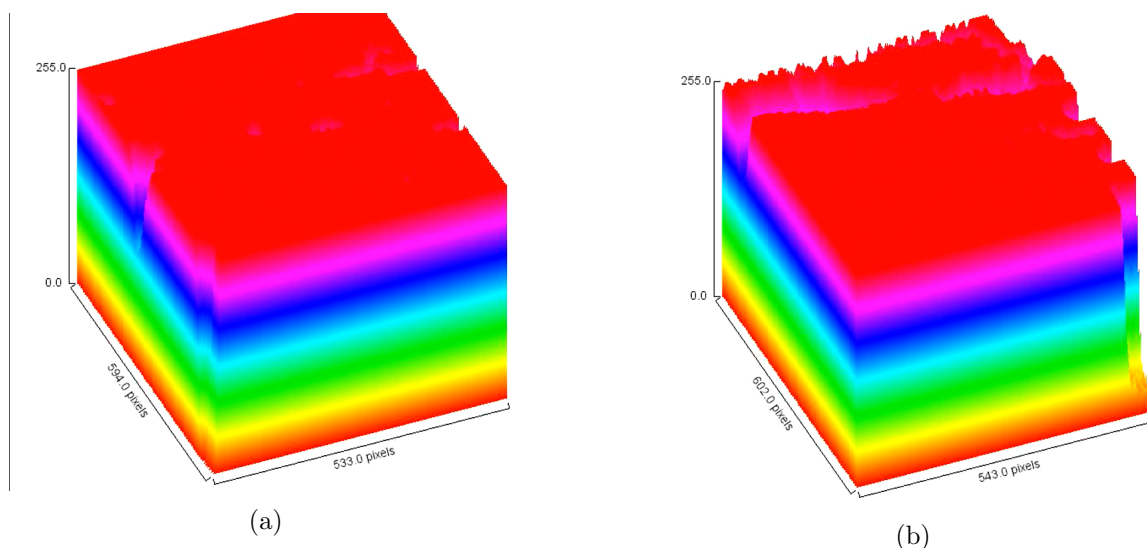


Figure 15: Last photograph of the 3D surface plots from the BW25133 strains with R100-1 plasmid. On the left the 180503 strain and on the right the day 180505 strain.

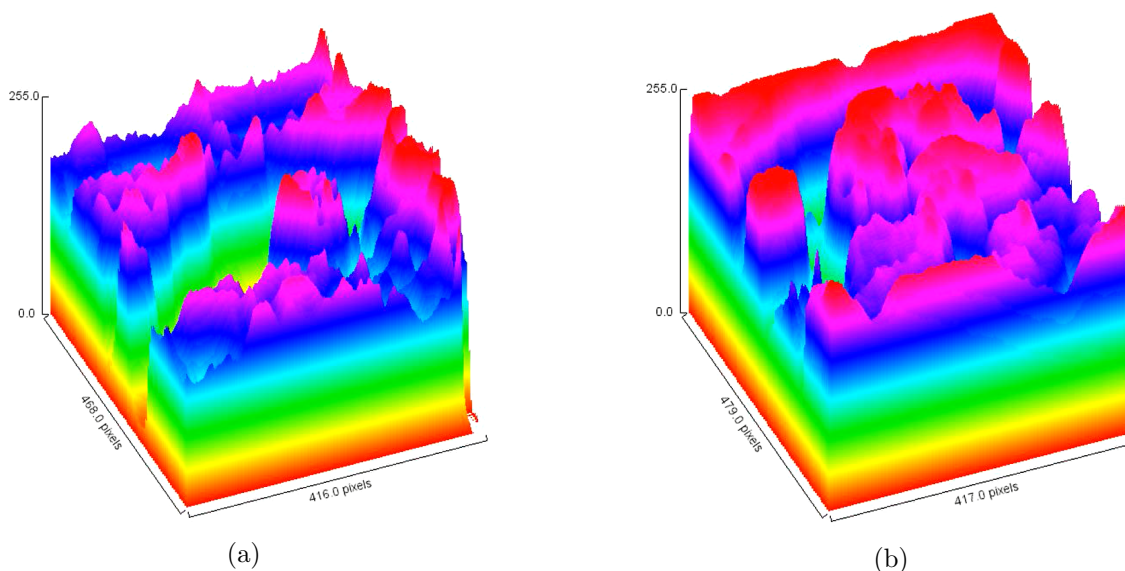


Figure 16: Last photograph of the 3D surface plots from the BW25133 strains with R100-1 plasmid and the 2-HDA inhibitor. The 180518 strain is on the left and the 180522 is on the right.

As said in the previously, the density of the biofilms was measured and represented into a graph, which is shown in Fig.18. The bacterial density can be studied as it grows during the time of the trial and the effect of the R100-1 plasmid and 2-HDA COIN are compared to each other and the negative control group as the bacteria multiply.

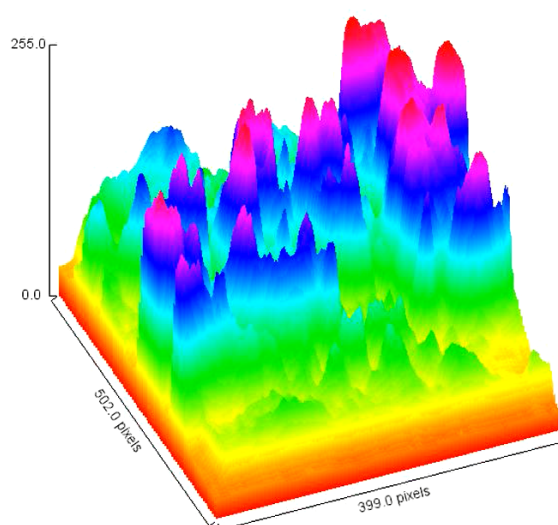


Figure 17: Last photograph of the 3D surface plots from the 180517 control group of BW25133 strain.

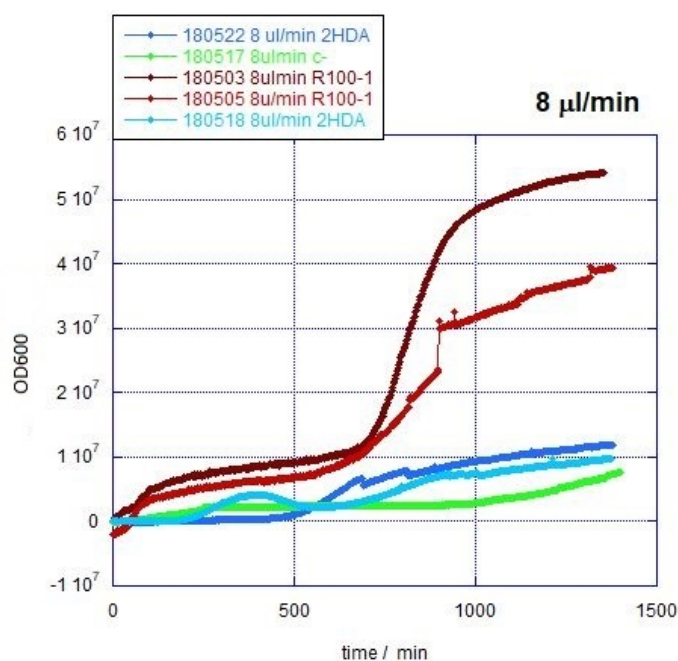


Figure 18: Representation of the optical density (OD) at 600 nm of the biofilms inside the microfluidic chip during the time (in minutes) when the flux was $8 \mu\text{l}/\text{min}$. In red, the strains with R100-1 conjugative plasmid are shown. In blue, the strain with the 2-HDA conjugative inhibitor are observed and, in green, the control group is displayed.

4.2 Biofilms grown at $10 \mu\text{l} / \text{min}$

In this part, the results of the bacterial evolution of the BW25133 strain when it was submitted to a continuous flux of $10 \mu\text{l}/\text{min}$ will be shown. The sequence of photographs taken every 3.15 h approximately of the biofilm evolution submitted to the R100-1 conjugative

plasmid, the 2-HDA COIN are represented in Fig. 19, with the the strain of the control group, respectively. In Fig. 20 to 22 the last photographs of the surface plots acquired from all of the experiments are shown.

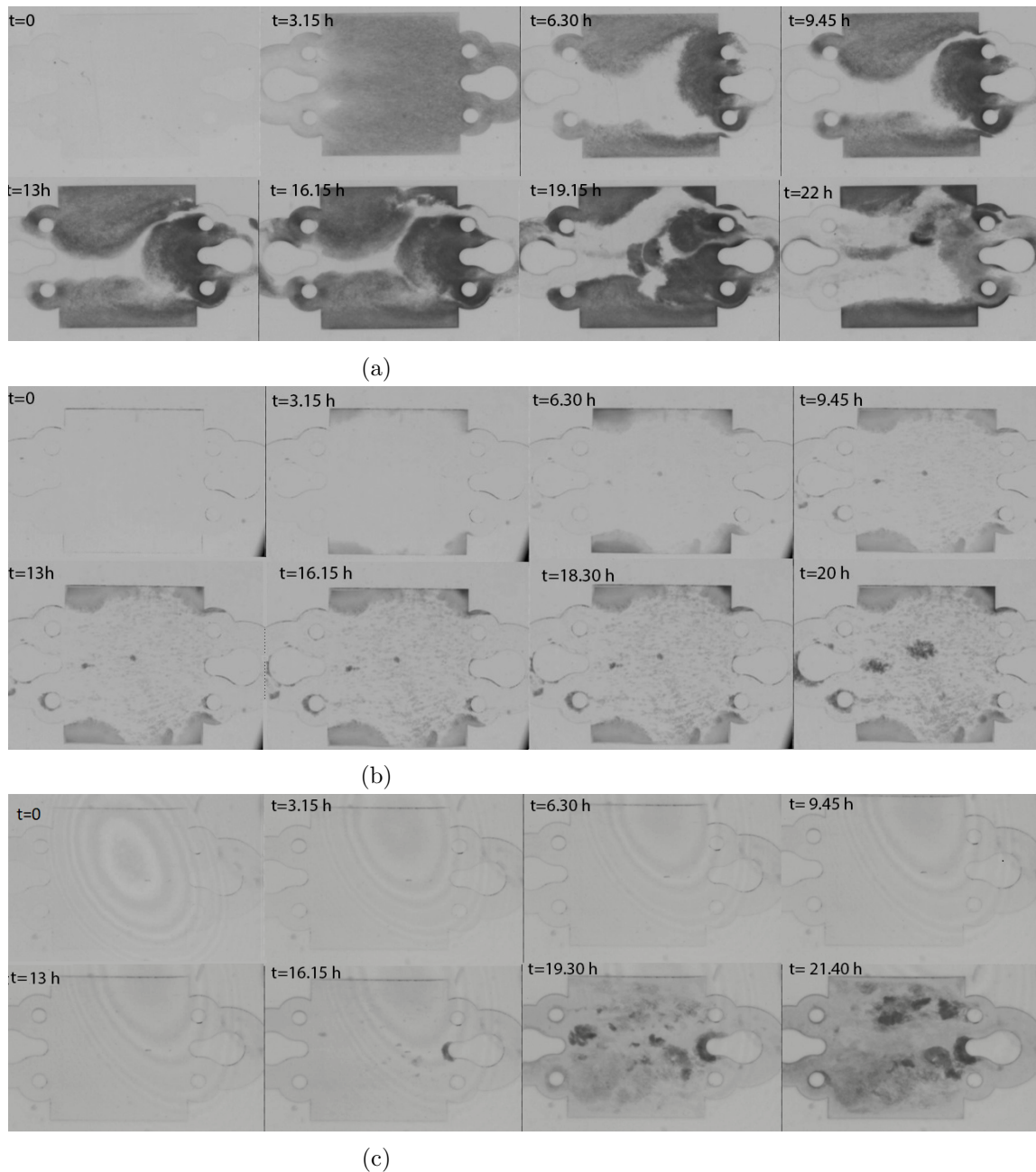


Figure 19: Combination of 8 photographs taken every 3.15 hours approximately from BW25513 strains with : (a) R100-1 conjugative plasmid, (b) 2-HDA conjugative inhibitor and (c) control group subjected to a $10 \mu\text{l}/\text{min}$ flux.

The density of the evolution of the biofilms was also plotted against time, where one can compare the effect of the R100-1 plasmid, 2-HDA COIN against the negative control groups,

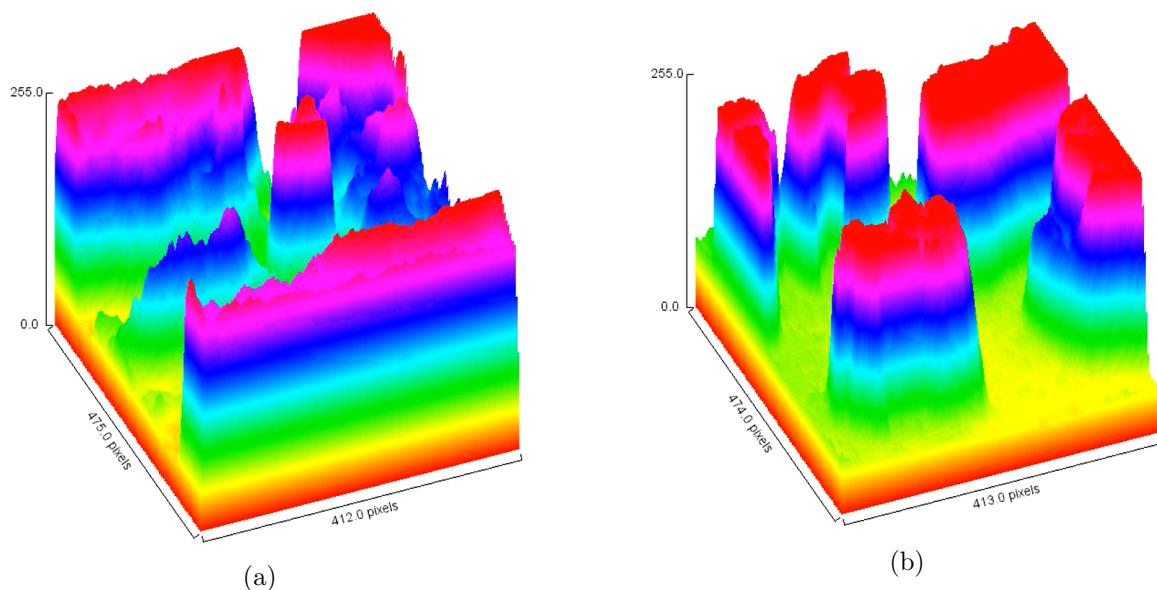


Figure 20: Last photograph of the 3D surface plots from the BW25133 strains with R100-1 plasmid. On the left the strain of 180528 and on the right on the day 180529.

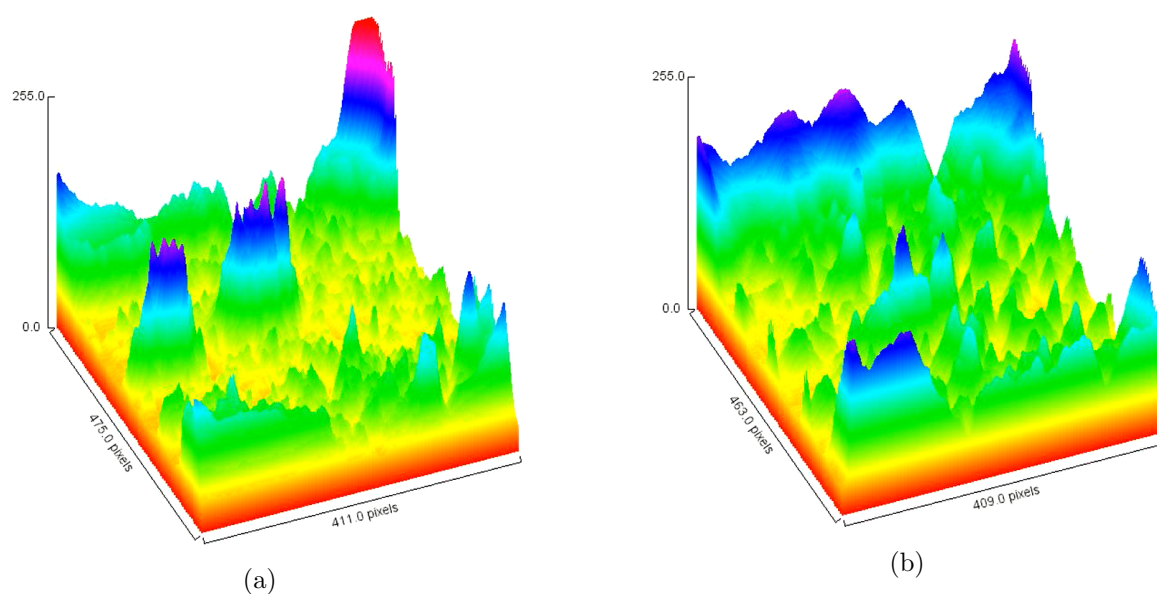


Figure 21: Last photograph of the 3D surface plots from the BW25133 strains with R100-1 plasmid and the 2-HDA inhibitor. On the left the 180530 experiment and 180531 on the right.

in Fig. 23.

Also, Fig. 18 and 23 are represented together to observe the differences the flux velocity created in the development of the biofilms, in Fig. 24.

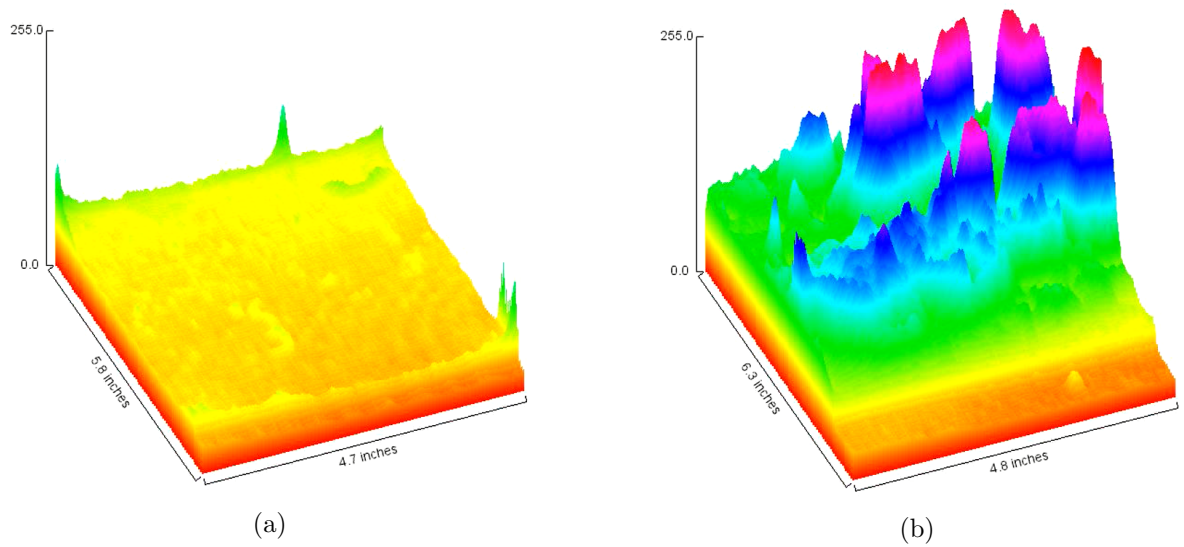


Figure 22: Last photograph of the 3D surface plots from the BW25133 control groups . On the left the strain of 180604 and on the right on the day 180607.

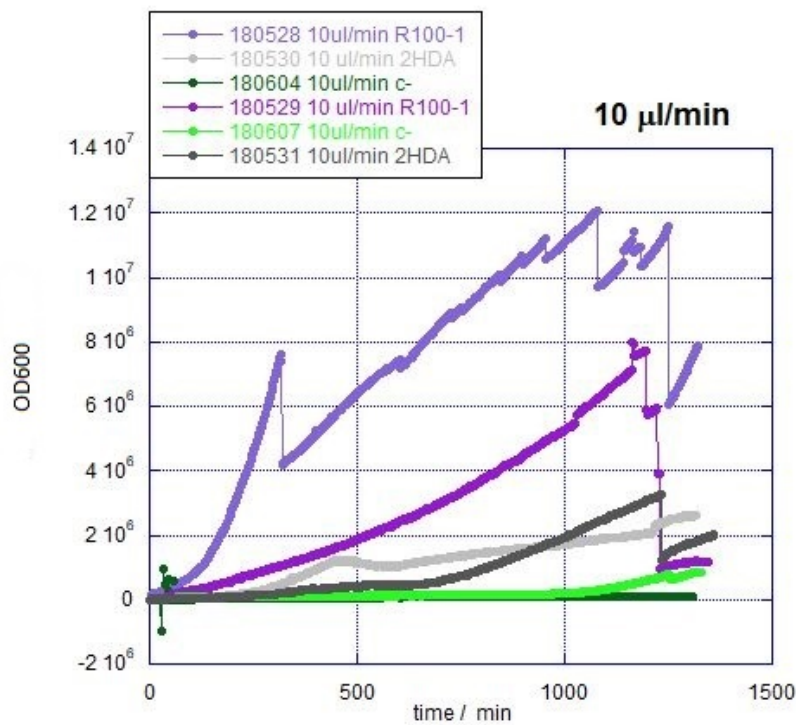
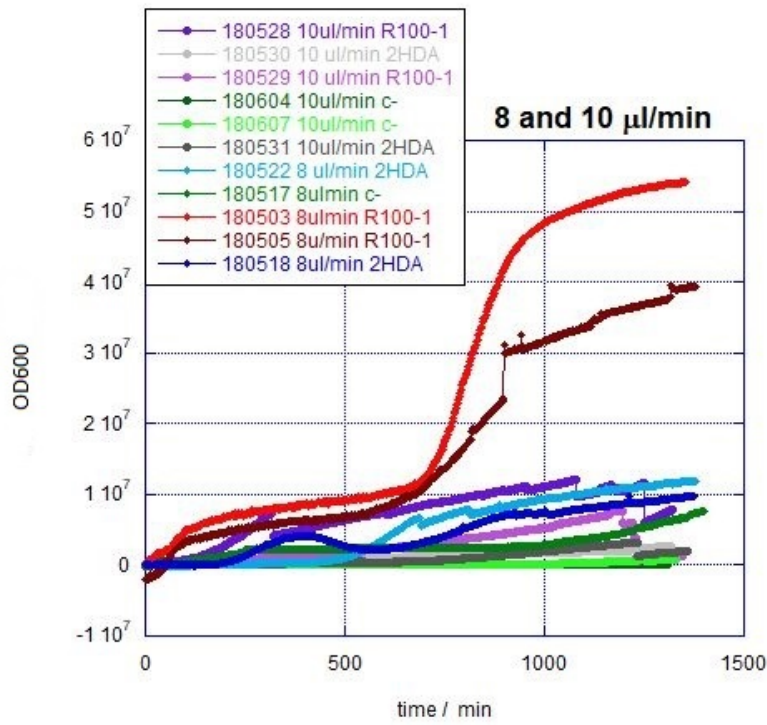
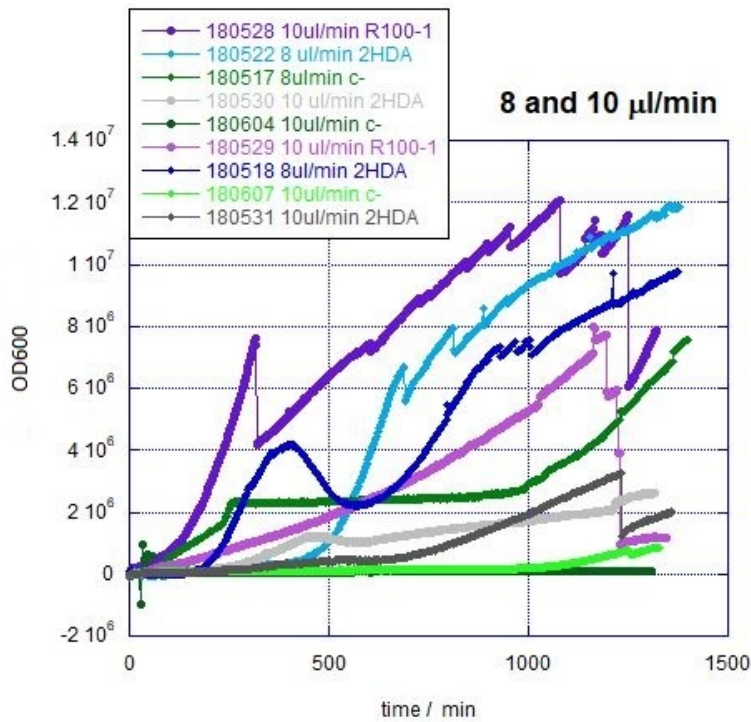


Figure 23: Representation of the optical density (OD) at 600 nm of the biofilms inside the microfluidic chip during the time (in minutes) when the flux was 10 μl/min. In purple, the strains with R100-1 conjugative plasmid are shown, in grey the strain with the 2-HDA conjugative inhibitor are seen and in green the control group are displayed.



(a)



(b)

Figure 24: Comparative graphs of the evolution of optical density the biofilms grown at 8 and 10 $\mu\text{l} / \text{min}$ seen in Fig. 18 and 23. The color chart is the same as in the figures. In (a) all of the curves from both fluxes are observed and in (b) all of them except the R100-1 in 8 $\mu\text{l} / \text{min}$ to see the differences in the section 0 - $1.2 \cdot 10^7$ clearer.

5 Discussion

In this work we have developed a experimental setup for the quantitation of biofilm formation in microfluidic chambers. We have analyzed biofilm formation at two different flow regimes, analyzing whether the conjugation inhibitor 2-HDA was effective preventing biofilm formation.

As stated before, this studies prime objective is to see the effect of the conjugative inhibitor 2-HDA on the growth of the biofilms. This purpose is easily observed in the strains subjected to a $8 \mu\text{l}/\text{min}$ flux, specially in Fig. 14 and 18. At $8 \mu\text{l}/\text{min}$, biofilm formation in the sample containing the conjugative plasmid and no inhibitor was apparent at $t=6.30$ h. Treatment with 2-HDA delayed biofilm formation for approximately 3 more hours. Moreover, biofilm intensity in the treated sample was substantially lower, as shown in Figure 23. Control experiments (containing bacteria without plasmid) also formed biofilm, but formation was severely delayed and reached lower densities.

Fig 18 shows that the BW25113 + R100-1 strains reach up to a density of $(4.7 \pm 0.7) \cdot 10^7$ and the BW25113 + 2-HDA + R100-1 strains reach to a density of $(1.1 \pm 0.2) \cdot 10^7$, which means the evolution of the biofilm drops to $(23 \pm 5) \%$. It is also seen in the graph that the evolution of strains with the COIN are very similar to the growth of the control group (in green). They have a discrepancy of 29 and 50%, which in this case is very low. In this figure, we see that the biofilms begin increase exponentially min $t \approx 700 \text{ min} = 11.6 \text{ h}$. In this time the bacteria are growing linearly and gathering nutrients until they can begin to multiply in large numbers. The exponential growth seems to stop in $t \approx 1000 \text{ min} = 16.6 \text{ h}$ where it seems to reach a maximum, where the bacteria have little space to grow, as one can also see in Fig. 19a. The biofilm on the exponential growth increases its density by more than double the original value: on the 180503 strain experiment ends in $5.5 \cdot 10^7$ which is 325% of the original value. On the 180505, the density of the strain goes from 3.49 to $4 \cdot 10^7$, a 227% of the original value.

Biofilms grew in an exponential fashion. However there are points in the videos in which large chunks of biofilm detach from the surface and are washed away by the flow. These events appear as sudden decreases in integral intensity in Figures 18 and 23. Biofilm breakup happened usually generally at the end of the experiment, when bacterial growth had almost

blocked the entire chamber. Flow obstruction in the chamber increases differential pressure between the inlet and the outlet of the chamber. This increase in the flow pressure finally rips off large biofilm chunks. In some videos it is apparent that the flow has been able to carve a gorge throughout the biofilm.

On the other hand, the strains with the 2-HDA COIN do not grow as much. By comparing Fig. 15 and 16 we see that the surface plots do not end with the same density, where the strains with the inhibitor do not reach a high density. Also, we can see that the density of the strains with 2-HDA increases their original density slightly, by $\approx 60\%$ in both cases.

Comparing the R100-1 strains with the 2-HDA treatment we see that the density of the biofilms have dropped considerably. Considering the experiment 180518, the difference between the plasmid strains 180503 and 180505 is of 80 and 75 %, respectively and with the experiment 180522 the discrepancy is of 78 and 70%. In other words, it prevents biofilm formation at a $(75 \pm 5)\%$. Proving that at "slow" fluxes the conjugative inhibitor is very efficient towards the biofilm formation restriction.

The biofilms that were under the influence of $10 \mu\text{l} / \text{min}$ grew less than the when the bacteria were under a slower flux.

In Fig. 19, the R100-1 plasmid on the second photograph, a biofilm base is formed. It is not dense, but it covers most of the chip. In the next photograph, $t=3.15$ h later, the current has not only separated the biofilm from the bottom of the chip creating a pathway for which it can pass, but also it has gathered most of the biofilm at the end of the chip increasing its density. From this stage, the biofilm grows according to the current, the size of the biofilms grows vertically and horizontally, but the biofilm that goes through the "river" gets carried away, which can also lead to a change in the currents path. On the other hand, the biofilm formed with the 2-HDA COIN and in the negative control group are much smaller, in size and density. With the 2-HDA, the biofilm grew specially in the borders of the chip, where the flow is much smaller because under a laminar flow regime, the speed of the flow decreases as we approach the border. Therefore, corners and borders of the chamber experience less dragging forces, facilitating bacterial attachment. Treatment with 2-HDA thus prevented biofilm growth in places of the chip directly affected by the flow. For example, some biofilm seeds were detected at $t=6.30$ h in the center of the chamber. Growth of these seeds, how-

ever, is severely delayed, compared to the growth rates exhibited by the untreated sample. When 2-HDA was present biofilm patches in the center of the chamber reached small sizes. In the control group, we see that the biofilms start to appear after 16 h of incubation under the flow, but they evolution quite fast creating, a small baseline and also larger biofilms in the center of the chip.

By seeing Fig. 23 the biofilms with the conjugative plasmid grew much less than the same bacteria at a lower rate and the strains with the COIN are similar to the negative control group. Here, the bacteria with the plasmid grow by a (160 ± 10) %.

In addition the 2-HDA works as well as in the $8 \mu\text{l}/\text{min}$, where, comparing the R100-1 and the inhibitor growth lines, we see that the experiment made on the 30th the percentage of biofilm was reduced by 73 and 60 % when compared with the experiments done on the 28th and 29th, and the difference of those two days are of 78 and 68 % compared to the experiment performed on the 31st. At both flow rates bacterial densities were reduced by approximately (70 ± 8) % by 2-HDA treatment. In the low flow regime this decrease was mainly due to less dense biofilm, although it still covered most of the fluidic chamber. At high flow rate the decrease was mainly due to entire areas of the chamber being biofilm-free. Overall, data indicated that 2-HDA successfully inhibited biofilm formation at both flow rates.

The effect of the flux velocity can be assessed by comparing the figures 15 to 22, in which we can see that the peaks of the spectrum in the $8 \mu\text{l}$ and $10 \mu\text{l}/\text{min}$ do not reach the same heights. To confirm this, in Fig. 24a one can see that the bacterial density of the $8 \mu\text{l}/\text{min}$ strains are bigger than the strains that grew under the $10 \mu\text{l}/\text{min}$. Observing Fig. 24b we can see that the density of the $10 \mu\text{l}$ bacterial strains have a similar density as the control group of the $8 \mu\text{l}/\text{min}$. Here the difference between these 4 strains are between 15 and 30%, which is very close in comparison with the other strains.

Finally, comparing the control groups in Fig. 24 one observes there is a large difference between them, whilst the difference in the flux is only $2 \mu\text{l}/\text{min}$. The difference between them is by a factor of 8. Which is even more pronounced because in the $10 \mu\text{l}/\text{min}$ experiments, there is hardly any growth in the negative control group. This data and the comparisons between the untreated samples revealed the critical role of the flux intensity in biofilm formation. It seems likely that there is a certain threshold upon which bacterial attachment

becomes increasingly more difficult. Biofilm formation thus depends on flow rates, and assessing the role of 2-HDA preventing it requires further analysis at different flow regimes. In order to fully evaluate the efficiency of this treatment preventing the formation of bacterial biofilms, a systematic analysis with different strains and different flow rates is required. Our experimental setup and quantitation system allows such analysis, thus this work represents the first step in the endeavour of preventing biofilm attachment using conjugation inhibitors.

6 Conclusions

The 2-HDA conjugative inhibitor reduces the number of biofilm formations by 75 and 69 percent in a continuous flow environment, depending on the flux velocity. At slower currents the inhibitor has a better chance of working against the biofilm, thus lowering the formation up to 3/4. This would mean that by studying the inhibitors, a possible solution for the biofilm formation in bodies.

Also, as predicted, the flux velocity is also a large factor in the formation of biofilms. By increasing a little the velocity of the current, the bacteria are not able to obtain as many nutrients, reducing the density by more than half as well or it can affect the biofilm by tearing it from the surface.

7 Acknowledgements

I would like to thank everyone in the 2.03 and 0.03 laboratories in the IBBTEC for their kindness, specially Carolina Palencia Gándara for her patience and all of her help and Ana Cuevas for showing me how to work in a biology laboratory. Also to Victor Campa for the FIJI macro that helped me obtain the optical density from the images.

8 References

- [1] C. Beloin, A. Roux and J.M Ghigo (2008) *Escherichia coli* Biofilms Curr Top Microbiol Immunol **322**: 249-289
- [2] C. Beloin, S. Renard, J.M. Ghigo (2014) *Novel approaches to combat bacterial biofilms* Current opinion in Pharmacology **18**, 61-68
- [3] C. Saenz, Harvard Medical School (2015) *Silanization of Photoresist Master Protocol* INFORMATION FOR USERS-PROTOCOLS & SAFETY, Microfluidics, microfluidics and microfabrication facility.
- [4] D. Huh, Y. Torisawa, G.A. Hamilton, H.J.Kim and D. E. Ingber (2012) *Microengineered physiological biomimicry: Organs on Chips Lab on a chip* **12**, 2156-2164
- [5] D. Qin, Y. Xia, J. A. Rogers, R. J. Jackman, x. M. Zhao, G. M. Whitesides (1998) *Microfabrication, Microstructures and Microsystems* Topics in Current Chemistry **194**, 1-20
- [6] E. Cabezón, F. de la Cruz, I. Arechaga (2017) *Conjugation Inhibitors and Their Potential Use to Prevent Dissemination of Antibiotic Resistance Genes in Bacteria* Front Microbiol. **8**, 2329
- [7] G. Sharma, S. Sharma, P. Sharma, D. Chandola, S.Dang, S.Gupta and R.Gabrani (2016) *Escherichia coli* biofilm: development and therapeutic strategies Journal of Applied Microbiology **121**, 309-319
- [8] J. Kim, H.D. Park and S. Chung (2012) *Microfluidic approaches to bacterial biofilm formation* Molecules. **17**, 9818-9834
- [9] J. Kim, M. Hegde, S. Ho Kim, T. K. Wood and A. Jayaraman (2012) *A microfluidic device for high throughput bacterial biofilm studies* Lab on a chip **12**, 1157-1163
- [10] J.L. Song, K.H Au, K.T.Huynh and A. I Packman (2014) *Biofilm Responses to Smooth Flow Fields and Chemical Gradients in Novel Microfluidic Flow Cells* Biotechnology and

Bioengineering **111**, No 13, 598-607

[11] J.M Ghigo (2001) *Natural conjugative plasmids induce bacterial biofilm development* Nature **412**, 442-445

[12] L. Hall-Stoodley, J.W. Costerton and P. Stoodley (2004) *Bacterial biofilms: from the natural environment to infectious diseases* Nature Reviews **2**, 95-106

[13] M. Getino, D.J. Sanabria-Ríos, R. Fernández-López, J. Campos-Gómez, J. M. Sánchez-López, A. Fernández, N.M. Carballeira, F. de la Cruz (2015) *Synthetic Fatty Acids Prevent Plasmid-Mediated Horizontal Gene Transfer* Mbio **6** 5, 1-8

[14] National Center for Biotechnology Information. PubChem Compound Database, CID=151047, <https://pubchem.ncbi.nlm.nih.gov/compound/151047> (accessed June 20, 2018). Modify Date: 2018-06-09

[15] A. San-Miguel & H. Lu (2013) *Microfluidics as a tool for C. elegans research* WormBook, ed. The C. elegans Research Community, WormBook.